BMC Cardiovascular Disorders

RESEARCH

Open Access

Tubercidin enhances apoptosis in serum-starved and hypoxic mouse cardiomyocytes by inducing nuclear speckle condensation

Guowen Shen[1,2†], Qingni Cheng[3†], Lunmin Liang[3†], Yaping Qin[1†], Yunzhu Cao[4†], Quanzhong Li[3*] and Shengjun Xiao[1*]

Abstract

Tubercidin, known for its antimicrobial, antiparasitic, and anticancer effects, faces clinical limitations due to adverse effects, especially cardiotoxicity risks for those with ischemic cardiomyopathy. This study aims to clarify the molecular pathways of Tubercidin-induced cardiotoxicity, focusing on nuclear speckles (NSs) disruption in cardiomyocytes under serum deprivation and/or hypoxia. To simulate ischemic cardiomyopathy in vitro, we utilized FMC84 and HL-1 murine cardiomyocyte cell lines, exposing them to conditions of serum limitation and/or hypoxia to evaluate the cardiotoxic impact of Tubercidin and the contributing mechanisms. Apoptosis was quantified using flow cytometry, NSs condensation was visualized via immunofluorescence with an anti-SC35 antibody, and the expression levels of key apoptotic transcripts (RFFL, RIF1, and RNF144B) were analyzed by RT-PCR. Our findings revealed that Tubercidin significantly increased apoptosis in both HL-1 and FMC84 cell lines under conditions mimicking serum deprivation (21% O2 with 1% FBS), hypoxia (1% O2 with 10% FBS), or a combination of both. Furthermore, Tubercidin treatment led to a pronounced enlargement of NSs, as detected by immunofluorescence. Concurrently, we documented significant alterations in the expression of critical apoptotic regulatory genes, implying that Tubercidin may modulate the apoptotic pathway in stressed cardiomyocytes. It is hypothesized that Tubercidin induces NSs condensation, affecting alternative splicing of cell death genes, potentially worsening ischemic cardiomyocytes' damage. Therefore, a cautious clinical use of Tubercidin for ischemic cardiomyopathy patients is advised to reduce cardiotoxicity risks.

Keywords Tubercidin, Apoptosis, Hypoxia, Nuclear speckles, Mouse Cardiomyocytes

† Guowen Shen, Qingni Cheng, Lunmin Liang, Yaping Qin and Yunzhu Cao contributed equally to this work.

*Correspondence:
Quanzhong Li
drquanzhongli@glmc.edu.cn
Shengjun Xiao
xiaoshengjun@glmc.edu.cn
[1] Department of Pathology, The Second Affiliated Hospital of Guilin Medical University, Guilin 541199, China
[2] Department of Anesthesiology, The People's Hospital of Guangxi Zhuang Autonomous Region, Nanning 530021, China
[3] Department of Cardiology, Guangxi Health Commission Key Laboratory of Basic Research in Sphingolipid Metabolism Related Diseases, the Affiliated Hospital of Guilin Medical University, Guilin 541001, China
[4] Department of Physiology, Faculty of Basic Medical Sciences, Guilin Medical University, Guilin 541199, China

Introduction

Tubercidin, an adenosine analog derived from Streptomyces tubercidicus, possesses a broad spectrum of pharmacological activities, exerting a potent inhibitory influence on diverse microorganisms, including bacteria, fungi, viruses, and protozoa [1]. Moreover, this compound has demonstrated promise as a chemotherapeutic agent for tumor treatment [2]. Upon cellular uptake through nucleoside transporters, Tubercidin undergoes intracellular phosphorylation to generate mono-, di-, and triphosphate forms that competitively inhibit adenosine nucleotides, thereby disrupting polymerase activity and subsequently halting DNA replication, RNA transcription, and protein synthesis [3, 4]. Additionally, structural modifications of Tubercidin have been shown to confer inhibitory effects on adenosine kinase [5].

The clinical deployment of Tubercidin is significantly limited by its considerable hepatotoxicity, nephrotoxicity, and cardiotoxicity, especially in individuals with cardiac comorbidities such as ischemic cardiomyopathy [6]. Therefore, deciphering the molecular pathways leading to its cardiotoxic effects is essential for devising strategies to alleviate these adverse outcomes. In the context of schistosomiasis, combination therapies have been employed to ameliorate the toxicity profile and reduce patient side effects [7]. Furthermore, chemical modification of Tubercidin has been investigated as a means to diminish its toxicity [8]. Despite these efforts, a thorough understanding of Tubercidin's toxicity mechanisms remains critical for enhancing its clinical safety profile.

Nuclear speckles (NSs) are RNA-binding protein-rich nuclear bodies, numbering approximately 20 to 30 per eukaryotic nucleus [9]. They are populated by a multitude of SR (Serine/Arginine-rich) proteins, which are pivotal in pre-mRNA splicing, mRNA transport, RNA stability, and translation [10]. Consequently, NSs serve as key assembly and storage sites for pre-mRNA splicing machinery [10]. During eukaryotic RNA splicing, SR proteins operate as essential splicing factors, in conjunction with snRNPs (small nuclear ribonucleoproteins) and other factors, to bind specific RNA sequences, identify splice sites, and facilitate both constitutive and alternative splicing [11]. The SR proteins are also instrumental in regulating apoptosis through the alternative splicing of genes associated with cell death [12], a process that is dependent on NSs [13]. To date, over ten SR protein varieties have been identified, with SRSF2 (Serine/Arginine-rich splicing factor 2), also known as SC35 (Splicing Component, 35 KDa), being a critical member of the serine/arginine (SR)-rich family of pre-mRNA splicing factors and a central constituent of NSs [14].

Tubercidin has been observed to perturb the assembly of NSs and consequently disrupt mRNA processing. Following Tubercidin exposure, poly (A)+RNAs dispersed throughout the nucleoplasm undergo decay, whereas SC35-labeled NSs persist in a condensed state [15]. This suggests that Tubercidin specifically impairs mRNA processing within NSs without disassembling these condensed nuclear subcompartments.

NSs are known to form under various stress conditions, including hypoxia and serum starvation, with their RNA processing events presumed to aid in cellular stress survival. Therefore, the disruption of these RNA processing events by Tubercidin, including mRNA splicing, is hypothesized to augment cardiomyocyte toxicity in individuals with ischemic heart diseases. Utilizing murine cardiomyocytes, this study provides evidence that Tubercidin induces the condensation of NSs and exacerbates apoptosis under hypoxic and/or serum-starved conditions. These findings suggest a cautious approach to the clinical use of Tubercidin in patients with ischemic cardiomyopathy.

Materials and methods

Maintenance of cardiomyocyte cell cultures

The HL-1 cell line, derived from mouse atrial cardiomyocytes, was sourced from Cellcook (Guangzhou, China) and maintained in a customized Claycomb medium (Sigma-Aldrich). This medium was fortified with 10% fetal bovine serum (FBS; Gibco), 4 mM L-glutamine, 0.1 mM noradrenaline, and an antibiotic–antimycotic mix (100 U/mL penicillin and 100 μg/mL streptomycin) to support cell viability and prevent contamination. The FMC84 cell line, which models mouse ventricular cardiomyocytes, was provided by Jennio Biotech (GuangZhou, China) and cultured in high glucose Dulbecco's Modified Eagle Medium (DMEM; Gibco) supplemented with the same additives as the HL-1 medium. Both cell lines were housed in a humidified incubator set at 37 °C with a 5% CO_2 atmosphere to maintain homeostatic culture conditions. Cellular experiments were performed during the exponential growth phase to ensure the cells exhibited consistent growth kinetics and biochemical responses.

Quantification of apoptosis induced by tubercidin

The cells were divided into three experimental groups based on the duration of exposure to Tubercidin at a concentration of 5 μg/mL, which was selected based on evidence from prior studies showing its effectiveness in modulating cellular responses [16, 17]. Additionally, a control group of cells not exposed to Tubercidin was included for comparison. Once the cells reached 80% confluence in a 10 cm diameter dish, they were exposed to Tubercidin for 1, 3, or 6 h. Following this exposure, the cells, along with the supernatant fractions, were harvested and then centrifuged at 1000 rpm for 5 min

to form a pellet. The pellets were washed twice with ice-cold PBS to remove culture medium components. Subsequently, cells were stained with Annexin V-FITC and PI according to the Cell Apoptosis Kit protocol (LIFE iLAB BIO, China), incubated in the dark for 15 min at room temperature, and analyzed using a flow cytometer (Invitrogen) to differentiate viable (Annexin V-FITC negative/PI negative), early apoptotic (Annexin V-FITC positive/PI negative), and late apoptotic or necrotic (Annexin V-FITC positive/PI positive) cells, thereby characterizing the apoptotic response over time. Each experiment was repeated three times to ensure the reliability and reproducibility of the results. Statistical evaluation included a one-way analysis of variance, succeeded by Tukey post hoc comparisons.

Immunofluorescence assay and measurement of nuclear speckle diameter and number using laser confocal microscopy

Cells were seeded onto glass coverslips placed in 24-well plates and allowed to reach 70–80% confluence. Then the cells treated with Tubercidin for 6 h. After PBS rinses and 15-min fixation with 4% PFA, cells were permeabilized with 0.5% Triton X-100. Following three PBST washes, cells were blocked with 10% FBS for 30 min and incubated overnight at 4 °C with a 1:200 diluted mouse anti-SC35 primary antibody (Novus Biologicals, USA). The next day, following three PBST washes, cells received a 1-h incubation with a 1:100 diluted Alexa 488-labeled goat anti-mouse IgG (ZSGD-BIO, China). Nuclei were stained with DAPI (4',6-diamidino-2-phenylindole) for 5 min, and coverslips were mounted using ProLong Gold Antifade Reagent (Thermo Fisher Scientific, USA). Nuclear speckles (NSs) were visualized and quantified using a Zeiss LSM 880 laser confocal microscope with Airyscan technology (Carl Zeiss AG, Oberkochen, Germany). Confocal images were acquired using a × 63 oil immersion objective with a numerical aperture of 1.4. Z-stack images were taken at 0.5 μm intervals to capture the entire depth of the NSs. The number and diameter of nuclear bodies were quantified using image analysis software Zeiss Zen Blue by setting a threshold for fluorescence intensity that distinguished NSs from the background. The software automatically counted the number of nuclear bodies and measured their diameter based on the area covered by the fluorescence signal. Data were analyzed from at least 30 randomly chosen fields per condition from three independent experiments. Statistical analysis was performed using one-way analysis of variance (ANOVA), and differences were considered significant at $P < 0.05$.

Gene expression analysis by RT-PCR

Total RNA was isolated from cells using TRIZOL Reagent (Sigma) and reverse-transcribed into cDNA (1 μg input) with the Reverse Transcription Kit (Biosharp, China). Subsequent RT-PCR employed M5 HiPer plus Taq HiFi PCR mix (Mei5 Biotechnology) for amplification. Specific primer pairs for GAPDH (5'-CGCCTGGAGAAACCTGC-3' and 5'-CGCCTGGAGAAACCTGC-3'), RNF144B (5'-CTCCAAGAGTGCCAGTGTATC-3' and 5'-CCATGTCAGGACAAGTGATAGG-3'), RIF1 (5'-CGTATGACTGGAGAAGAAGG-3' and 5'-GCCTACAATGAAGAAACCAAT-3'), and RFFL (5'-AGTACCTACTGAGGATGAGACC-3' and 5'-CGGTCAGGCCTTCAATGT-3') were used, with GAPDH serving as a normalizer. The PCR conditions were optimized as follows: an initial denaturation at 95 °C for 3 min, followed by 30 cycles of 95 °C for 1 min, 60 °C for 30 s, and 72 °C for 30 s, with a final extension at 72 °C for 10 min to ensure complete synthesis of the target amplicons. Each experiment was repeated three times to ensure the reliability and reproducibility of the results.

Statistical analysis

Experiments were conducted in triplicate, and data were subjected to statistical analysis using IBM SPSS Statistics 22.0. Differences among groups were assessed via one-way analysis of variance (ANOVA) followed by post hoc tests for pairwise comparisons, where appropriate. A *p*-value of less than 0.05 was considered to denote statistical significance. Data visualization was performed using GraphPad Prism 8.0 to create informative and publication-quality graphs and charts.

Results

Enhanced apoptosis in mouse cardiomyocytes following tubercidin exposure under ischemic and hypoxic conditions

This investigation revealed that exposure to Tubercidin significantly elevated apoptosis levels in FMC84 (Fig. 1) and HL-1 (Fig. 2) cardiomyocytes under conditions mimicking ischemia and hypoxia (Table 1). Under normoxic conditions with standard serum, Tubercidin (5 μg/mL) initiated apoptosis in FMC84 cells by 6 h and consistently increased apoptosis in HL-1 cells throughout the 1 to 6-h monitoring period. The apoptotic effect was markedly intensified under conditions of serum deprivation and hypoxia, with both cell lines exhibiting increased apoptosis at each monitored time point (1 h, 3 h, 6 h). The concomitant presence of serum starvation and hypoxia was found to have a synergistic effect, significantly amplifying the cardiotoxic impact of Tubercidin and leading to a pronounced increase in apoptosis. These results

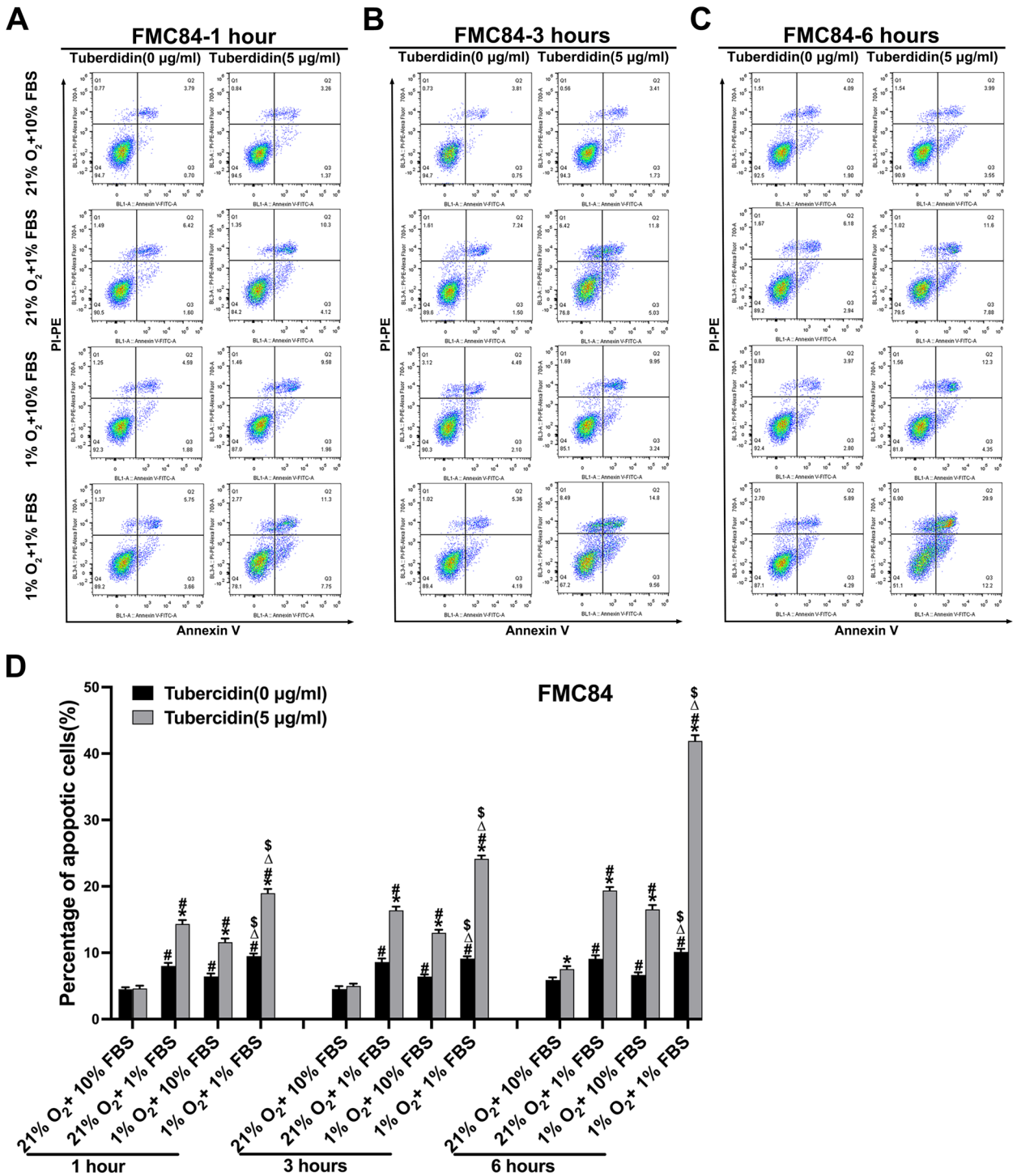

Fig. 1 Tubercidin treatment increased apoptosis of mouse cardiomyocyte FMC84 under the stress of serum starvation or/and hypoxia. **A** Flow cytometry analysis showing apoptosis of FMC84 cells after 1 h of Tubercidin treatment under different conditions. **B** Flow cytometry analysis showing apoptosis of FMC84 cells after 3 h of Tubercidin treatment under different conditions. **C** Flow cytometry analysis showing apoptosis of FMC84 cells after 6 h of Tubercidin treatment under different conditions. **D** Quantification of apoptotic cells across all treatment groups. Tubercidin treatment significantly elevated apoptosis levels under conditions of serum starvation and/or hypoxia compared to untreated controls. Furthermore, a more pronounced increase in apoptosis was observed when cells were subjected to both serum starvation and hypoxia simultaneously, as opposed to either condition alone. *, Compared with Tubercidin (0 μg/ml), $P < 0.05$; #, Compared with 21% O_2 + 10% FBS, $P < 0.05$; Δ, Compared with 21% O_2 + 1% FBS, $P < 0.05$; $, Compared with 1% O_2 + 10% FBS, $P < 0.05$

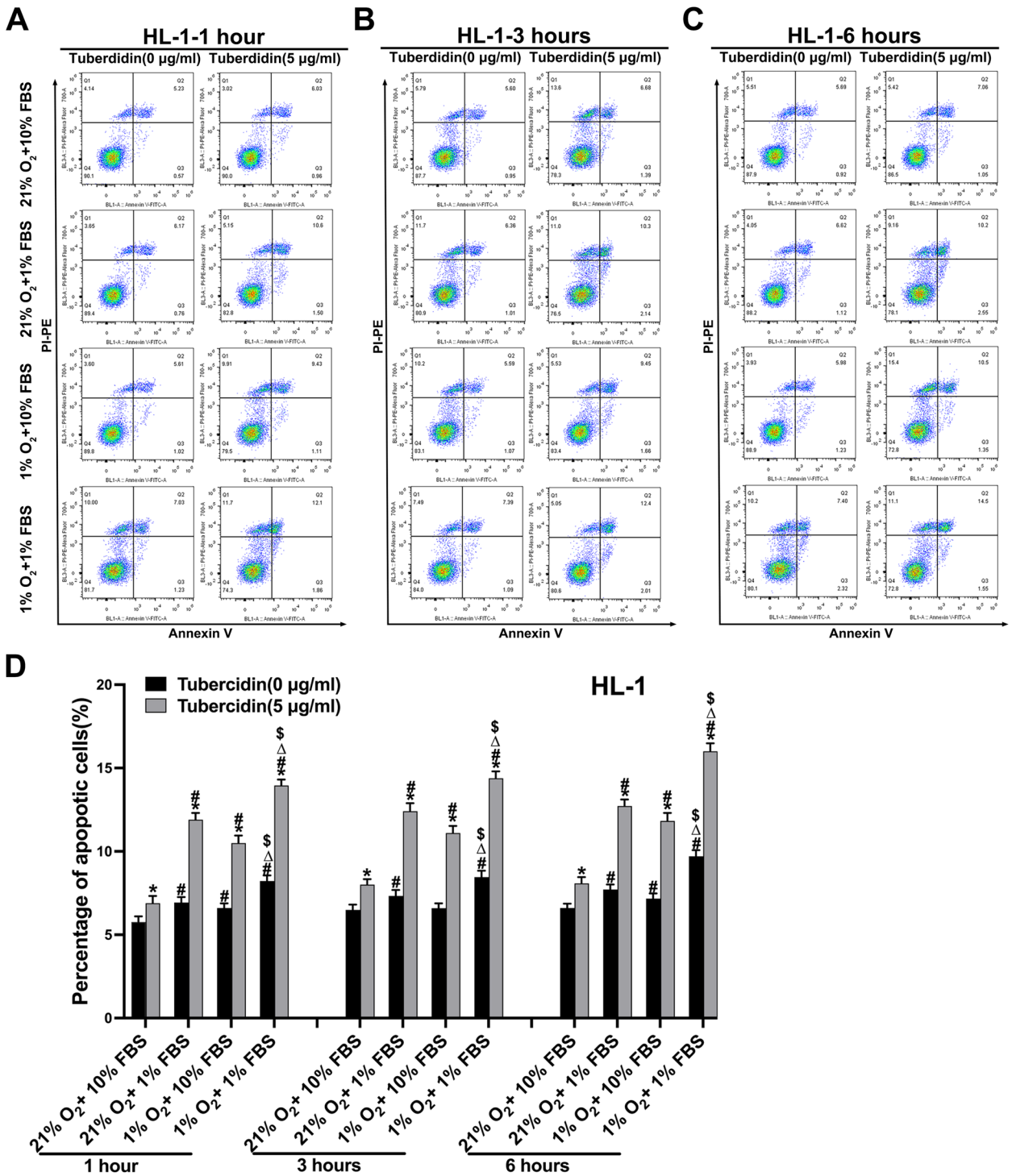

Fig. 2 Tubercidin treatment increased apoptosis of mouse cardiomyocyte HL-1 under the stress of serum starvation or/and hypoxia. **A** Flow cytometry analysis showing apoptosis of HL-1 cells after 1 h of Tubercidin treatment under different conditions. **B** Flow cytometry analysis showing apoptosis of HL-1 cells after 3 h of Tubercidin treatment under different conditions. **C** Flow cytometry analysis showing apoptosis of HL-1 cells after 6 h of Tubercidin treatment under different conditions. **D** Quantification of apoptotic cells across all treatment groups. Tubercidin treatment significantly elevated apoptosis levels under conditions of serum starvation and/or hypoxia compared to untreated controls. Furthermore, a more pronounced increase in apoptosis was observed when cells were subjected to both serum starvation and hypoxia simultaneously, as opposed to either condition alone. *, Compared with Tubercidin (0 μg/ml), $P < 0.05$; #, Compared with 21% O_2 + 10% FBS, $P < 0.05$; Δ, Compared with 21% O_2 + 1% FBS, $P < 0.05$; $, Compared with 1% O_2 + 10% FBS, $P < 0.05$

Table 1 The impact of Tubercidin on cell apoptosis of FMC84 and HL-1 cells under stress of serum starvation or/and hypoxia (Mean ± SD, $n = 3$)

Groups	Apoptotic rate(%)					
	FMC84			HL-1		
	1 h	3 h	6 h	1 h	3 h	6 h
21% O_2 + 10% FBS						
Tubercidin (0 μg/ml)	4.52 ± 0.30	4.54 ± 0.43	5.89 ± 0.41	5.76 ± 0.35	6.49 ± 0.32	6.60 ± 0.27
Tubercidin (5 μg/ml)	4.62 ± 0.43	5.00 ± 0.36	7.53 ± 0.46*	6.89 ± 0.44*	8.00 ± 0.33*	8.08 ± 0.37*
21% O_2 + 1% FBS						
Tubercidin (0 μg/ml)	8.00 ± 0.48#	8.60 ± 0.54#	9.10 ± 0.51#	6.93 ± 0.33#	7.33 ± 0.36#	7.71 ± 0.30#
Tubercidin (5 μg/ml)	14.33 ± 0.60*#	16.38 ± 0.58*#	19.37 ± 0.52*#	11.9 ± 0.41*#	12.41 ± 0.48*#	12.72 ± 0.39*#
1% O_2 + 10% FBS						
Tubercidin (0 μg/ml)	6.43 ± 0.46#	6.42 ± 0.31#	6.65 ± 0.39#	6.60 ± 0.28#	6.59 ± 0.29	7.17 ± 0.31#
Tubercidin (5 μg/ml)	11.59 ± 0.57*#	13.00 ± 0.46*#	16.54 ± 0.65*#	10.50 ± 0.45*#	11.10 ± 0.43*#	11.83 ± 0.47*#
1% O_2 + 1% FBS						
Tubercidin (0 μg/ml)	9.50 ± 0.40#Δ$	9.12 ± 0.35#Δ$	10.13 ± 0.46#Δ$	8.22 ± 0.34#Δ$	8.46 ± 0.38#Δ$	9.71 ± 0.36#Δ$
Tubercidin (5 μg/ml)	18.98 ± 0.62*#Δ$	24.16 ± 0.48*#Δ$	41.90 ± 0.87*#Δ$	13.95 ± 0.36*#Δ$	14.39 ± 0.41*#Δ$	16.00 ± 0.48*#Δ$

*, Compared with Tubercidin (0 μg/ml), $P < 0.05$; #, Compared with 21% O_2 + 10% FBS, $P < 0.05$

Δ, Compared with 21% O_2 + 1% FBS, $P < 0.05$; $, Compared with 1% O_2 + 10% FBS, $P < 0.05$

underscore the heightened sensitivity of cardiomyocytes to the apoptotic effects of Tubercidin when subjected to combined stressors, providing insights into the mechanisms of drug-induced cardiotoxicity within the context of ischemic heart disease.

Tubercidin-induced condensation of SC35-labeled nuclear speckles under ischemic and hypoxic stress

The influence of Tubercidin on the structural integrity of nuclear speckles (NSs) was assessed through immunofluorescence staining with an anti-SC35 antibody. Our findings indicate that after 6 h, a timepoint chosen based on the maximal condensation of NSs (19), cells exposed to both serum starvation and hypoxia exhibited a pronounced increase in NS size and a concomitant decrease in their number, suggesting a synergistic impact of these stressors on NSs assembly. Moreover, Tubercidin treatment under conditions of serum starvation or hypoxia, individually or in combination, consistently resulted in enlarged SC35-labeled NSs with a reduced count in FMC84 and HL-1 cells (Fig. 3A & B). These observations imply that Tubercidin may induce condensation and fragmentation of NSs, which could subsequently impair the RNA processing functions associated with these cellular structures.

Regulation of anti-apoptotic gene expression by tubercidin in conditions of ischemia and hypoxia

This investigation assessed how Tubercidin affects the expression of key anti-apoptotic genes—RFFL, RNF144B, and RIF1—under ischemic and/or hypoxic stress. Given the role of exon skipping in altering the levels of major transcripts within nuclear speckles, we hypothesized that Tubercidin might modulate these transcripts. Using RT-PCR, we quantified the expression of the genes.

In FMC84 cells, hypoxia, and serum starvation independently induced RFFL expression, which was then significantly diminished by Tubercidin, pointing to a potential disruption in splicing regulation (Fig. 4A). In HL-1 cells, however, RFFL expression did not significantly vary with stress or Tubercidin exposure, indicating cell-specific responses to these conditions (Fig. 5A). RIF1 expression followed a similar pattern, being upregulated by stress, and downregulated by Tubercidin in both cell lines (Figs. 4B and 5B). RNF144B expression in FMC84 cells was slightly increased by stress and significantly enhanced by Tubercidin, especially under normoxic conditions and serum starvation (Fig. 4C). In contrast, RNF144B expression was not detected in HL-1 cells (Fig. 5C), underscoring the cell type dependency of these effects.

These findings suggest that Tubercidin can alter the expression of anti-apoptotic genes, likely through the interference with splicing processes associated with nuclear speckles, with the extent of this effect being dependent on both the cell type and the combined stress of ischemia and hypoxia.

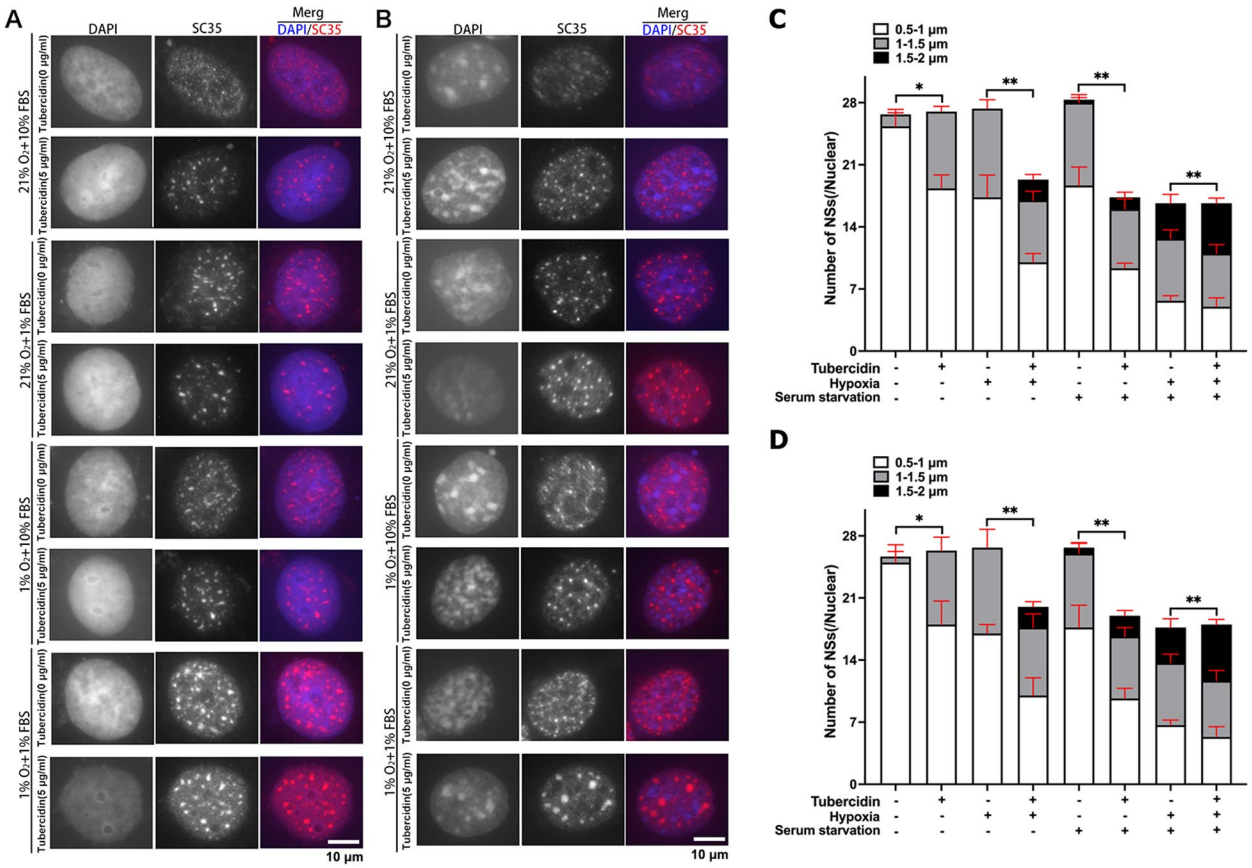

Fig. 3 Tubercidin induces aggregation and enlargement of SC35-labeled nuclear speckles (NSs) in mouse cardiomyocytes. **A** Confocal microscopy images showing SC35-labeled NSs in FMC84 cardiomyocytes after 6 h of Tubercidin treatment. Merged images highlight the colocalization of SC35 (green) with DAPI-stained nuclei (blue). Tubercidin treatment led to a decrease in the number of SC35-labeled NSs and an increase in their size compared to control cells under serum starvation and/or hypoxia. **B** Confocal microscopy images showing SC35-labeled NSs in HL-1 cardiomyocytes after 6 h of Tubercidin treatment. Similar to FMC84 cells, Tubercidin treatment resulted in fewer but larger SC35-labeled NSs compared to control cells under serum starvation and/or hypoxia. Bar, 10 μm. **C** Quantitative analysis of the number of SC35-labeled NSs condensates in FMC84 cells and (**D**) HL-1 cells treated with Tubercidin for 6 h. The number of NSs significantly decreased and the size of NSs, with more condensates falling into larger size categories (1.5–2 μm) in FMC84 cells and HL-1 cells exposed to Tubercidin compared to controls under serum starvation and/or hypoxia

Discussion

Tubercidin, a purine ribonucleoside analog, exhibits broad-spectrum antimicrobial activity against bacteria, fungi, and parasites, including Mycobacterium tuberculosis and Streptococcus faecalis [1]. It also shows antiviral potential against SARS-CoV-2 [18, 19] and influenza virus [20]. However, its clinical application is limited by significant nephrotoxicity, which led to the discontinuation of trials for cancer chemotherapy. Consequently, research has focused on structural modifications to reduce its toxicity [21]. Nevertheless, the specific mechanisms underlying Tubercidin's toxicity remain unclear. Elucidating these mechanisms is crucial for further development and clinical application of the drug.

In addition to its antimetabolic effects, Tubercidin has been identified as a disruptor of nuclear speckle (NS) formation [15]. NSs are dynamic subnuclear structures enriched with RNA processing factors and poly(A)+RNAs, including mRNAs and non-coding RNAs [22]. These structures serve as hubs for RNA splicing, 3′ end processing, and other maturation steps, with key factors like RBBP6 anchoring these processes within the speckles [23]. NSs play a crucial role in both RNA processing and gene transcription by coupling these processes. They store nascent transcripts during transient transcriptional inhibition, facilitating efficient gene expression [14]. Additionally, RNA-binding proteins within NSs, such as RBM22, can directly interact with chromatin to regulate transcription initiation, elongation,

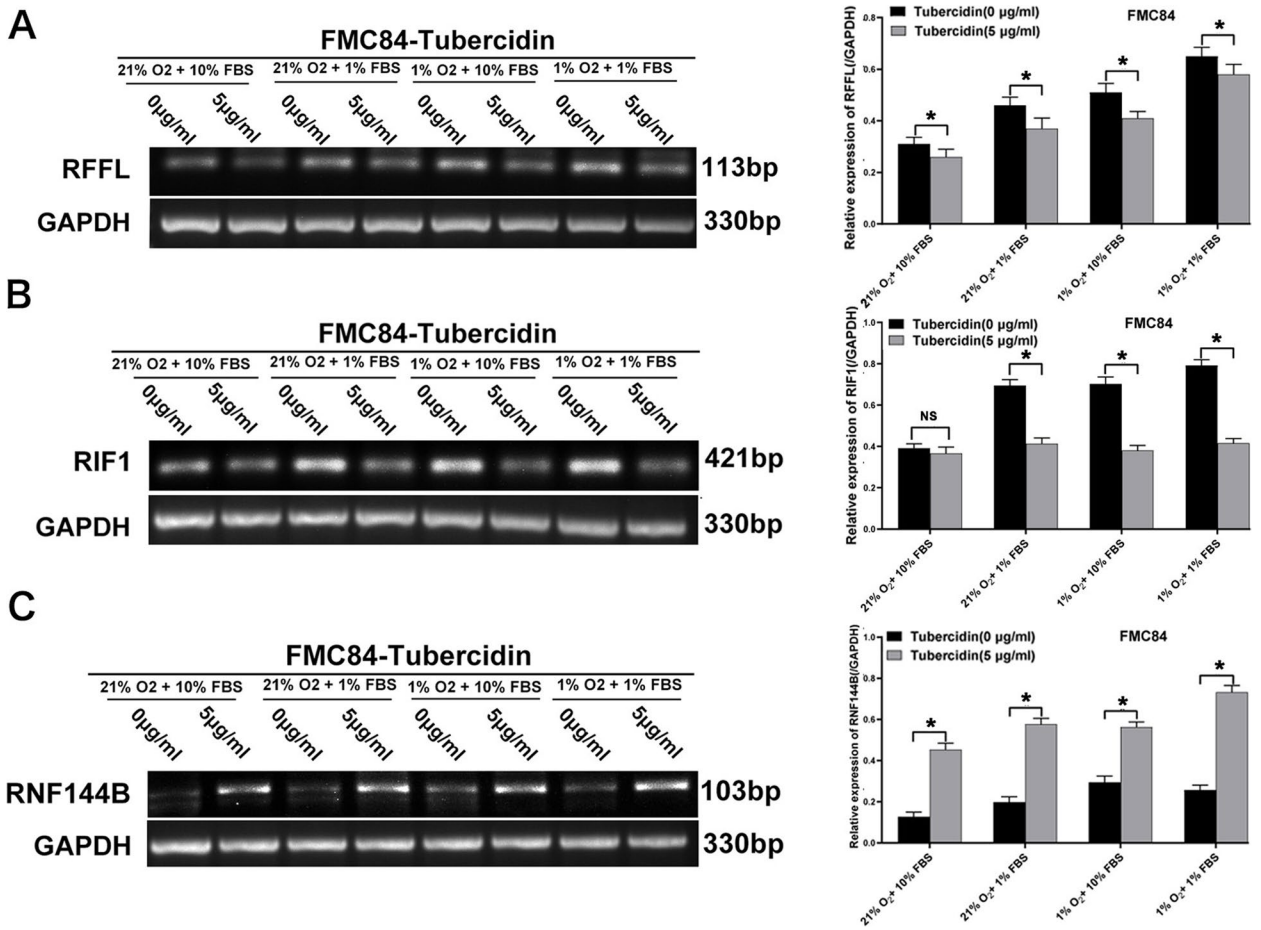

Fig. 4 Expression changes of key apoptosis-related genes in FMC84 cells after 6 h of Tubercidin treatment under varying oxygen and serum conditions. **A** Western blot analysis showing the relative expression levels of the antiapoptotic gene RFFL in FMC84 cells. After 6 h of Tubercidin treatment (5 μg/ml), the expression of RFFL significantly decreased across all conditions tested (21% O_2 + 10% FBS, 21% O_2 + 1% FBS, 1% O_2 + 10% FBS, 1% O_2 + 1% FBS) compared to the untreated controls. GAPDH was used as a loading control. **B** Western blot analysis showing the relative expression levels of the DNA repair and antiapoptotic gene RIF1 in FMC84 cells. The expression of RIF1 was significantly reduced after 6 h of Tubercidin treatment under all tested conditions compared to the untreated controls. GAPDH was used as a loading control. **C** Western blot analysis showing the relative expression levels of the proapoptotic gene RNF144B in FMC84 cells. The expression of RNF144B was significantly increased after 6 h of Tubercidin treatment under all tested conditions compared to the untreated controls. GAPDH was used as a loading control. * Statistical significance compared to untreated controls ($P < 0.05$)

and termination [24]. This multifunctionality highlights the importance of NSs in orchestrating gene expression and cellular responses to transcriptional changes.

NSs have been implicated in various pathological and physiological processes, including inflammation, cancer, and metabolic diseases [10]. For instance, in cancer, alterations in NS organization have been linked to changes in gene expression and cellular metabolism that drive tumorigenesis [25]. In metabolic diseases, the reorganization of NSs can affect the expression of key metabolic genes, influencing cellular responses to metabolic stress [26]. Additionally, in ischemic conditions, the reorganization of nuclear speckles facilitates the recruitment of splicing factors and enhances the splicing of pre-mRNAs, including those of immediate early genes (IEGs) such as ZFP36 and FOS [27]. This dynamic remodeling of nuclear speckles under stress conditions suggests that they play a significant role in modulating gene expression and cellular responses to ischemia, which is relevant to the pathogenesis of ischemic heart disease. Our findings confirm that Tubercidin enhances cardiomyocyte apoptosis under conditions simulating ischemia and hypoxia, as evidenced by increased apoptosis in FMC84 and HL-1 cells (Figs. 1 & 2). This suggests that Tubercidin may exacerbate the cardiomyocyte toxicity associated with ischemic heart disease.

Under stress conditions, such as hypoxia, the reorganization of nuclear speckles can lead to changes in

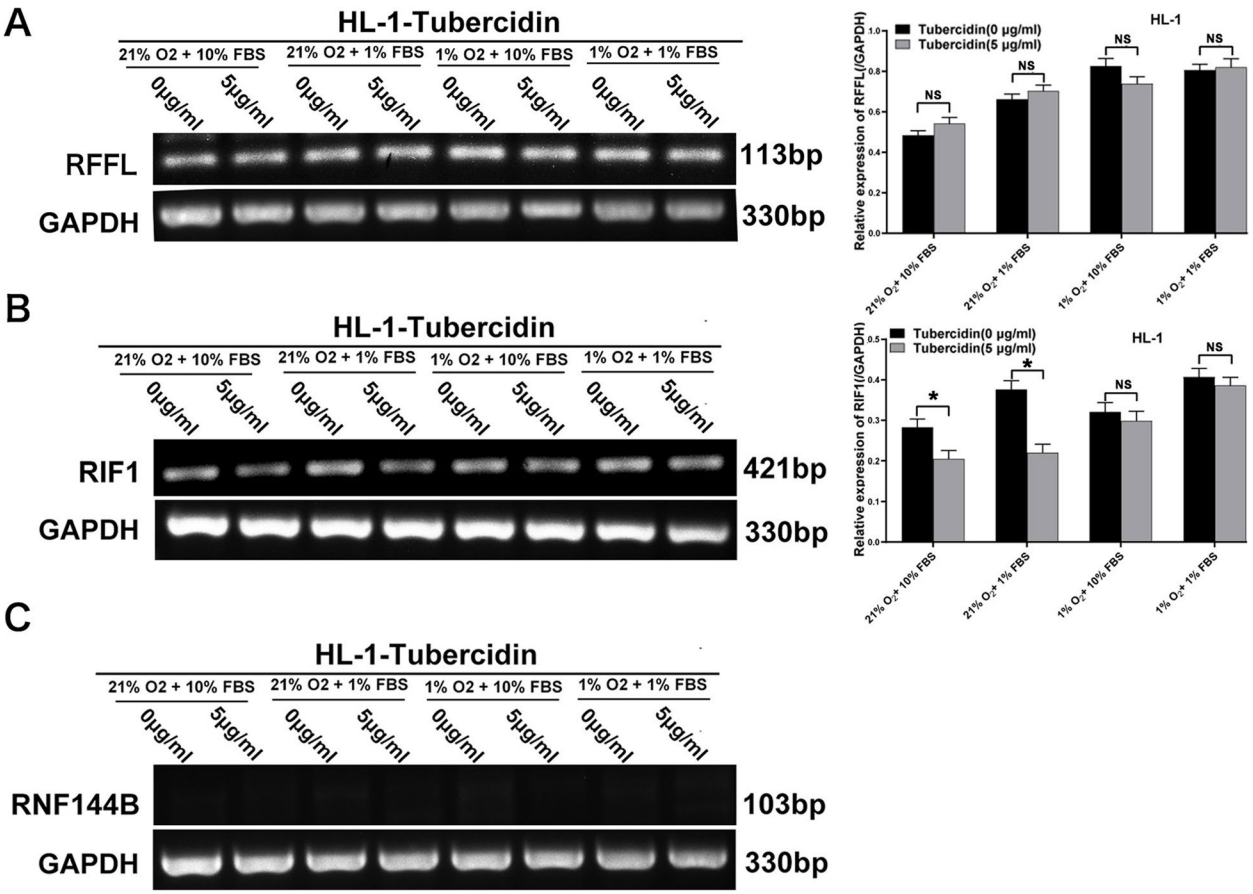

Fig. 5 Expression changes of key apoptosis-related genes in HL-1 cells after 6 h of Tubercidin treatment under varying oxygen and serum conditions. **A** Western blot analysis showing the relative expression levels of the antiapoptotic gene RFFL in HL-1 cells. After 6 h of Tubercidin treatment (5 μg/ml), the expression of RFFL significantly decreased across all conditions tested (21% O_2 + 10% FBS, 21% O_2 + 1% FBS, 1% O_2 + 10% FBS, 1% O_2 + 1% FBS) compared to the untreated controls. GAPDH was used as a loading control. **B** Western blot analysis showing the relative expression levels of the DNA repair and antiapoptotic gene RIF1 in HL-1 cells. The expression of RIF1 was significantly reduced after 6 h of Tubercidin treatment under all tested conditions compared to the untreated controls. GAPDH was used as a loading control. **C** Western blot analysis showing the relative expression levels of the proapoptotic gene RNF144B in HL-1 cells. The expression of RNF144B was significantly increased after 6 h of Tubercidin treatment under all tested conditions compared to the untreated controls. GAPDH was used as a loading control. * Statistical significance compared to untreated controls ($P < 0.05$)

alternative splicing patterns, thereby affecting the expression of apoptosis-related genes [28]. Similarly, other studies have shown that the dispersion of splicing factors from nuclear speckles, as induced by compounds like Tubercidin, can promote exon skipping in the alternative splicing of genes such as Clk1 [15]. This highlights the importance of nuclear speckles in maintaining the balance of splicing events and, consequently, the regulation of apoptosis-related gene expression.

Tubercidin's incorporation into nucleic acids disrupts normal RNA processing, leading to the condensation of NSs [15]. Our study further demonstrates that serum starvation and hypoxia alter the morphology of NSs in cardiomyocytes, increasing their size while reducing their number, as indicated by SC35 labeling. Tubercidin treatment exacerbates this condensation effect (Fig. 3). This disruption of NSs interferes with their critical functions in mRNA metabolism, including transcription and alternative splicing, ultimately resulting in transcriptome changes that correspond to cellular stress responses.

Nuclear speckles (NSs) are subnuclear compartments enriched with RNA processing factors and play a pivotal role in various aspects of RNA metabolism, including transcription, splicing, and polyadenylation [10]. Our unpublished data indicate that the expression of RFFL, RIF1, and RNF144B—genes associated with apoptosis—is altered by the knockdown of an NS component. RFFL, a ubiquitin-protein ligase, promotes the degradation of caspases and p53, thereby inhibiting apoptosis [29, 30]. RIF1, a regulator of DNA repair, suppresses apoptosis

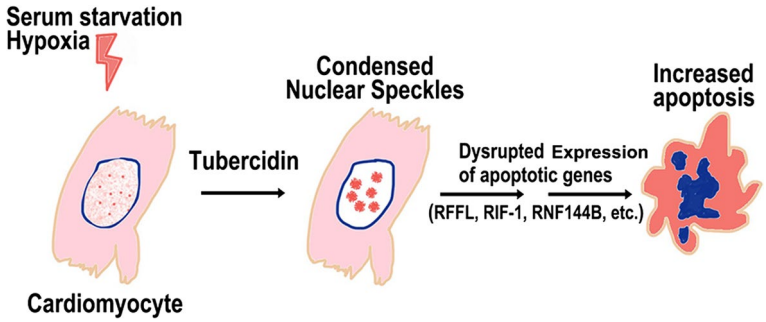

Fig. 6 Proposed mechanism of the cardiotoxicity induced by Tubercidin. This figure illustrates the proposed mechanism by which Tubercidin induces cardiotoxicity in cardiomyocytes under conditions of serum starvation and/or hypoxia. Tubercidin disrupts the normal function of nuclear speckles (NSs), which are critical for the regulation of mRNA metabolism, such as transcription and alternative splicing, affecting the expression of key apoptotic genes

under DNA damage conditions [31]. RNF144B, a mitochondrial ubiquitin-protein transferase, also negatively regulates apoptosis [32]. Our RT-qPCR analysis revealed that serum starvation and hypoxia upregulate RFFL and RIF1 while downregulating RNF144B, suggesting a stress response mechanism in cardiomyocytes that is linked to the broader RNA processing functions of NSs.

Conclusion

Tubercidin disrupted this stress-induced expression pattern, suggesting that it interferes with NSs-mediated regulation of apoptotic gene expression, potentially increasing cardiomyocyte toxicity under ischemic and hypoxic conditions (Fig. 6). These findings underscore the importance of considering Tubercidin's cardiotoxic potential, particularly in patients under stresses such as ischemic cardiomyopathy, where its clinical use should be approached with caution.

Supplementary Information

The online version contains supplementary material available at https://doi.org/10.1186/s12872-025-04661-4.

Supplementary Material 1.

Acknowledgements
Not applicable.

Authors' contributions
Guowen Shen contributed to data curation, investigation, validation, and was a major writer of the original draft. Qingni Cheng engaged in investigation and data curation, and played a role in drafting the manuscript. Lunmin Liang participated in investigation, data curation, visualization, and co-wrote the original draft. Yue Fu was involved in investigation and data curation, also contributing to the original draft. Yunzhu Cao assisted with investigation and data curation. Xiaoling Zhang was instrumental in conceptualizing the study, developing methodology, and was a key figure in software utilization, validation, visualization, and drafting the original manuscript. Quanzhong Li was pivotal in conceptualization, formal analysis, securing funding, project administration, and provided critical review and editing of the manuscript. Shengjun Xiao played a significant role in conceptualization, data curation, securing funding, and was a major contributor to the original writing, review, and editing of the manuscript.

Funding
The Guangxi BaGui Scholars Special Project and the Guilin City Science Research and Technological Development Program, No. 2020011204–3. The Basic Scientific Research Ability Improvement Project for Young and Middle-aged Teachers of Guangxi Colleges and Universities, No. 2023KY0507. Guangxi Key Research and Development Plan, No.GuiKe AB24010096. Guangxi Science and Technology Base and Talent Special Project, No.GuiKe AD24999032.

Data availability
Data is provided within the manuscript and/or supplementary information files.

Declarations

Ethics approval and consent to participate
Not applicable.

Consent for publication
Not applicable.

Competing interests
The authors declare no competing interests.

Received: 16 December 2024 Accepted: 12 March 2025
Published online: 22 March 2025

References

1. Swain SS, Paidesetty SK, Padhy RN. Antibacterial, antifungal and antimycobacterial compounds from cyanobacteria. Biomed Pharmacother. 2017;90:760–76.
2. Chen J, Barrett L, Lin Z, Kendrick S, Mu S, Dai L, Qin Z. Identification of natural compounds tubercidin and lycorine HCl against small-cell lung cancer and BCAT1 as a therapeutic target. J Cell Mol Med. 2022;26(9):2557–65.
3. Paterson AR, Harley ER, Cass CE. Inward fluxes of adenosine in erythrocytes and cultured cells measured by a quenched-flow method. Biochem J. 1984;224(3):1001–8.
4. Bloch A, Mihich E, Leonard RJ, Nichol CA. Studies on the biologic activity and mode of action of 7-deazainosine. Cancer Res. 1969;29:110–5.
5. Chauhan C, Kraemer A, Knapp S, Windheim M, Kotlyarov A, Menon MB, Gaestel M. 5-Iodotubercidin sensitizes cells to RIPK1-dependent necroptosis by interfering with NFκB signaling. Cell Death Discov. 2023;9(1):262.

6. Kolassa N, Jakobs ES, Buzzell GR, Paterson AR. Manipulation of toxicity and tissue distribution of tubercidin in mice by nitrobenzylthioinosine 5'-monophosphate. Biochem Pharmacol. 1982;31(10):1863–74.
7. Aoki JI, Yamashiro-Kanashiro EH, Ramos DC, Cotrim PC. Efficacy of the tubercidin antileishmania action associated with an inhibitor of the nucleoside transport. Parasitol Res. 2009;104(2):223–8.
8. Ouyang W, Huang H, Yang R, Ding H, Xiao Q. First total synthesis of 5'-O-α-d-glucopyranosyl tubercidin. Mar Drugs. 2020;18(8):398.
9. Faber GP, Nadav-Eliyahu S, Shav-Tal Y. Nuclear speckles - a driving force in gene expression. J Cell Sci. 2022;135(13):jcs259594.
10. Galganski L, Urbanek MO, Krzyzosiak WJ. Nuclear speckles: molecular organization, biological function and role in disease. Nucleic Acids Res. 2017;45(18):10350–68.
11. Li D, Yu W, Lai M. Targeting serine- and arginine-rich splicing factors to rectify aberrant alternative splicing. Drug Discov Today. 2023;28(9): 103691.
12. Stevens M, Oltean S. Modulation of the apoptosis gene Bcl-x function through alternative splicing. Front Genet. 2019;6(10):804.
13. Naro C, Barbagallo F, Chieffi P, Bourgeois CF, Paronetto MP, Sette C. The centrosomal kinase NEK2 is a novel splicing factor kinase involved in cell survival. Nucleic Acids Res. 2014;42(5):3218–27.
14. Ilık İA, Aktaş T. Nuclear speckles: dynamic hubs of gene expression regulation. FEBS J. 2022;289(22):7234–45.
15. Kurogi Y, Matsuo Y, Mihara Y, Yagi H, Shigaki-Miyamoto K, Toyota S, Azuma Y, Igarashi M, Tani T. Identification of a chemical inhibitor for nuclear speckle formation: implications for the function of nuclear speckles in regulation of alternative pre-mRNA splicing. Biochem Biophys Res Commun. 2014;446(1):119–24.
16. Inoue A, Tsugawa K, Tokunaga K, Takahashi KP, Uni S, Kimura M, Nishio K, Yamamoto N, Honda K, Watanabe T, Yamane H, Tani T. S1–1 nuclear domains: characterization and dynamics as a function of transcriptional activity. Biol Cell. 2008;100(9):523–35.
17. Wang LY, Xiao SJ, Kunimoto H, Tokunaga K, Kojima H, Kimura M, Yamamoto T, Yamamoto N, Zhao H, Nishio K, Tani T, Nakajima K, Sunami K, Inoue A. Sequestration of RBM10 in nuclear bodies: targeting sequences and biological significance. Int J Mol Sci. 2021;22(19): 10526.
18. Wang T, Zheng G, Chen Z, Wang Y, Zhao C, Li Y, Yuan Y, Duan H, Zhu H, Yang X, Li W, Du W, Li Y, Li D. Drug repurposing screens identify Tubercidin as a potent antiviral agent against porcine nidovirus infections. Virus Res. 2024;339: 199275.
19. Uemura K, Nobori H, Sato A, Sanaki T, Toba S, Sasaki M, Murai A, Saito-Tarashima N, Minakawa N, Orba Y, Kariwa H, Hall WW, Sawa H, Matsuda A, Maenaka K. 5-Hydroxymethyltubercidin exhibits potent antiviral activity against flaviviruses and coronaviruses, including SARS-CoV-2. iScience. 2021;24(10):103120.
20. Tsukamoto Y, Hiono T, Yamada S, Matsuno K, Faist A, Claff T, Hou J, Namasivayam V, Vom Hemdt A, Sugimoto S, Ng JY, Christensen MH, Tesfamariam YM, Wolter S, Juranek S, Zillinger T, Bauer S, Hirokawa T, Schmidt FI, Kochs G, Shimojima M, Huang YS, Pichlmair A, Kümmerer BM, Sakoda Y, Schlee M, Brunotte L, Müller CE, Igarashi M, Kato H. Inhibition of cellular RNA methyltransferase abrogates influenza virus capping and replication. Science. 2023;379(6632):586–91.
21. Liu Y, Gong R, Liu X, Zhang P, Zhang Q, Cai YS, Deng Z, Winkler M, Wu J, Chen W. Discovery and characterization of the tubercidin biosynthetic pathway from Streptomyces tubercidicus NBRC 13090. Microb Cell Fact. 2018;17(1):131.
22. Chen LL, Kim VN. Small and long non-coding RNAs: Past, present, and future. Cell. 2024;187(23):6451–85.
23. Yoon Y, Bournique E, Soles LV, Yin H, Chu HF, Yin C, Zhuang Y, Liu X, Liu L, Jeong J, Yu C, Valdez M, Tian L, Huang L, Shi X, Seelig G, Ding F, Tong L, Buisson R, Shi Y. RBBP6 anchors pre-mRNA 3'end processing to nuclear speckles for efficient gene expression. Mol Cell. 2025;S1097–2765(24):01033–5.
24. Du X, Qin W, Yang C, Dai L, San M, Xia Y, Zhou S, Wang M, Wu S, Zhang S, Zhou H, Li F, He F, Tang J, Chen JY, Zhou Y, Xiao R. RBM22 regulates RNA polymerase II 5' pausing, elongation rate, and termination by coordinating 7SK-P-TEFb complex and SPT5. Genome Biol. 2024;25(1):102.
25. Alexander KA, Yu R, Skuli N, Coffey NJ, Nguyen S, Faunce CL, Huang H, Dardani IP, Good AL, Lim J, Li CY, Biddle N, Joyce EF, Raj A, Lee D, Keith B, Simon MC, Berger SL. Nuclear speckles regulate functional programs in cancer. Nat Cell Biol. 2025. https://doi.org/10.1038/s41556-024-01570-0. Epub ahead of print. PMID: 39747580.
26. Musawi S, Donnio LM, Zhao Z, Magnani C, Rassinoux P, Binda O, Huang J, Jacquier A, Coudert L, Lomonte P, Martinat C, Schaeffer L, Mottet D, Côté J, Mari PO, Giglia-Mari G. Nucleolar reorganization after cellular stress is orchestrated by SMN shuttling between nuclear compartments. Nat Commun. 2023;14(1):7384.
27. Sung HM, Schott J, Boss P, Lehmann JA, Hardt MR, Lindner D, Messens J, Bogeski I, Ohler U, Stoecklin G. Stress-induced nuclear speckle reorganization is linked to activation of immediate early gene splicing. J Cell Biol. 2023;222(12): e202111151.
28. de Oliveira Freitas Machado C, Schafranek M, Brüggemann M, Hernández Cañás MC, Keller M, Di Liddo A, Brezski A, Blümel N, Arnold B, Bremm A, Wittig I, Jaé N, McNicoll F, Dimmeler S, Zarnack K, Müller-McNicoll M. Poison cassette exon splicing of SRSF6 regulates nuclear speckle dispersal and the response to hypoxia. Nucleic Acids Res. 2023;51(2):870-890.
29. Taniguchi S, Ono Y, Doi Y, Taniguchi S, Matsuura Y, Iwasaki A, Hirata N, Fukuda R, Inoue K, Yamaguchi M, Tashiro A, Egami D, Aoki S, Kondoh Y, Honda K, Osada H, Kumeta H, Saio T, Okiyoneda T. Identification of α-Tocopherol succinate as an RFFL-substrate interaction inhibitor inducing peripheral CFTR stabilization and apoptosis. Biochem Pharmacol. 2023;215: 115730.
30. Yang W, Dicker DT, Chen J, El-Deiry WS. CARPs enhance p53 turnover by degrading 14-3-3sigma and stabilizing MDM2. Cell Cycle. 2008;7(5):670–82.
31. Kabrani E, Rahjouei A, Berruezo-Llacuna M, Ebeling S, Saha T, Altwasser R, Delgado-Benito V, Pavri R, Di Virgilio M. RIF1 integrates DNA repair and transcriptional requirements during the establishment of humoral immune responses. Nat Commun. 2025;16(1):777.
32. Du L, Chen W, Li C, Cui Y, He Z. RNF144B stimulates the proliferation and inhibits the apoptosis of human spermatogonial stem cells via the FCER2/NOTCH2/HES1 pathway and its abnormality is associated with azoospermia. J Cell Physiol. 2022;237(9):3565–77.

Publisher's Note